Inorganic Chemistry

Article

pubs.acs.org/IC

Triple-Layered Perovskite Niobates $CaRNb_3O_{10}$ (R = La, Sm, Eu, Gd, Dy, Er, Yb, or Y): New Self-Activated Oxides

Lin Qin,[†] Donglei Wei,[‡,§] Yanlin Huang,*[,†] Sun Il Kim,[‡] Young Moon Yu,[§] and Hyo Jin Seo*[,§,‡]

[†]College of Chemistry, Chemical Engineering and Materials Science, Soochow University, Suzhou, Jiangsu 215123, China

[‡]Department of Physics and Interdisciplinary Program of Biomedical Engineering, Pukyong National University, Busan 608-737, Republic of Korea

[§]LED-Marin Convergence Technology R&BD Center, Pukyong National University, Busan 608-739, Republic of Korea

ABSTRACT: Niobates $CaRNb_3O_{10}$ (R = La, Sm, Eu, Gd, Dy, Er, Yb, or Y) were prepared by conventional high-temperature solid-state reaction. The formation of a single-phase compound with triple-layered perovskite-type structure was verified through X-ray diffraction (XRD) studies. The luminescence characteristics such as photoluminescence excitation and emission spectra, X-ray-excited luminescence (XEL), Stokes shift, decay curves, and color coordinates were investigated. The niobates can be efficiently excited by UV light and present luminescence behaviors with rich luminescence colors. Under excitation by ultraviolet radiation, $CaRNb_3O_{10}$ (R = La, Gd, Yb, or Y) exhibits strong blue luminescence due to the self-activation center of the octahedral NbO_6 groups, even at room temperature. For the materials of composition $CaRNb_3O_{10}$ (R = Sm, Eu, Dy, or Er), the excitation at the host band produces a characteristic luminescence of rare earth ions, indicating a host−guest energy transfer process. $CaRNb_3O_{10}$ (R = Eu) has the strongest luminescence intensity, which can be efficiently excited by near UV wavelength. It could be suggested to be a potential candidate for the application on near-UV excited white LEDs.

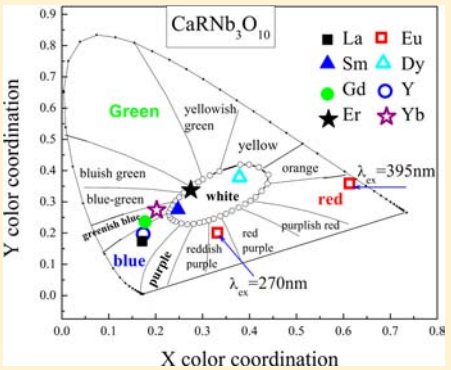

1. INTRODUCTION

The well-known perovskite structure ABX_3 and related structures have been intensively studied in modern solid state sciences.[1−8] Here A sites are large cations suited to dodecahedral coordination AO_{12} (A = K^+, Ba^{2+}, Ca^{2+}, Bi^{3+}, La^{3+}, etc.); B sites are occupied by small cations adaptive for octahedral coordination (B = Ti^{4+}, Ta^{5+}, Nb^{5+}, etc.), and X is an anion; Octahedral BX_6 groups link by the vertices and form three-dimensional frames. The layered perovskite-like structure built by two-dimensional single, double, triple, or more layers of octahedral-sharing vertices forms a very large group of versatile and interesting materials[9] and has been intensively investigated for the properties of dielectric,[10] superconductor,[11,12] colossal magnetic resistance,[13] thermoelectric,[14] luminescence,[15,16] magnetic and charge transport,[17] photocatalytic,[18] energy saving,[19] etc.

$MCa_2Nb_3O_{10}$ is one of the most important layered perovskites, which can be described by $M_m[A_{n-1}B_nO_{3n+1}]$[20] of the Dion−Jacobson-type oxides, where B corresponds to Nb or Ta(V), M can be an alkali-metal ion (K, Rb, or Cs) that neutralizes the negative layer charge, A represents an earth alkali ion (Ca or Sr), lead, bismuth, or lanthanides (La or Nd), and *n* indicates the number of NbO_6 octahedra chains that form the perovskite-like layer).[21] From a structural viewpoint, it consists of two-dimensional NbO_6 octahedral layers and M (usually K) ions, which locate at the interlayer region, can be replaced by simple cation in aqueous solution,[22] hydrogen ions,[23,24] organic cations,[25,26] etc. Consequently, this kind of material has attracted attention as a photocatalyst.[27−31] Moreover rare earth ions (REs) can be pillared in the triple perovskite layers. Ca^{2+} ions in the perovskite subcell can be replaced by rare earth metal ions such as La^{3+} to form $K_{1-x}Ca_{2-x}La_xNb_3O_{10}$ and $K_{1-x}Ca_{2-x}La_xNb_3O_{10}$ can be easily converted to $H_{1-x}Ca_{2-x}La_xNb_3O_{10}$ by ion exchange reaction.[28,32] The end member $LaCaNb_3O_{10}$, which contains no interlayer cations, is a novel layered perovskite oxide, being an *n* = 3 member of the series of $A_{n-1}B_nX_{3n+1}$.

Usually layered niobates can exhibit photoluminescence (PL) properties when excited in the UV region due to charge transfer (CT) transition in NbO_6 groups.[33] However, the $KCa_2Nb_3O_{10}$ matrix does not present emission at room or liquid nitrogen temperatures.[29] It is interesting that in $KCa_2Nb_3O_{10}$ the La^{3+} insertion in its structure produces a blue emitter compound at room temperature. This indicates that the electronic properties of the layered materials are modified by the lanthanide insertions. Bizeto et al.[29] reported the PL emission and excitation properties of Eu^{3+}-doped $KCa_2Nb_3O_{10}$ and concluded that there was an energy transfer process from the niobate matrix to activator (Eu^{3+}). Therefore, the layered perovskite is a potentially valuable host to realize luminescence from rich f−f transitions of RE ions.

In this work, niobates $CaRNb_3O_{10}$ (R = La, Sm, Eu, Gd, Dy, Er, Yb, or Y) with triple-layered perovskite-type structure were

Received: May 9, 2013
Published: August 26, 2013

reported as a kind of novel luminescence material. The crystal phase formation was verified by XRD measurements. The luminescence properties were investigated by PL excitation and emission spectra, decay curves, and color coordinates. Luminescence spectra under X-ray excitation were detected. This may be helpful in developing new luminescence materials in layered perovskites.

2. EXPERIMENTAL SECTION

Triple-layered perovskites $CaRNb_3O_{10}$ (R = La, Sm, Eu, Gd, Dy, Er, Yb, or Y) were synthesized using the solid-state reaction. The starting material was a stoichiometric mixture of $CaCO_3$, Nb_2O_5, and R_2O_3 (R = La, Sm, Eu, Gd, Dy, Er, Yb, or Y) with the purity of 99.99%. First, the mixture was thoroughly ball-milled using zirconia balls in plastic containers filled with ethanol for 24 h. Then the slurry was filtered and heated to 850 °C in an alumina crucible for 5−10 h. The obtained powder was ground again and then fired at 1300−1350 °C for 20−48 h twice.

The PL excitation and emission spectra were recorded on a Perkin-Elmer LS-50B luminescence spectrometer with Monk−Gillieson type monochromators and a xenon discharge lamp used as an excitation source. UV−vis diffuse reflectance spectra (UV-DRS) were measured on a UV−vis spectrophotometer (type Shimadzu, UV-2550). The X-ray excited luminescence (XEL) spectra were measured by an X-ray-excited spectrometer, FluorMain, where an F-30 movable X-ray tube (W anticathode target) was used as the X-ray source. The luminescence decay curves were recorded by the 500 MHz digital storage oscilloscope (Tektronics TDS754A). The samples were excited by the fourth harmonics (266 nm) of an Nd:YAG pulsed laser. All measurements were carried out at room temperature. The luminescence quantum efficiency (QE) was measured by a standard Edinburgh Instruments FS-920 spectrometer equipped with an Edinburgh instruments integrating sphere. The monochromator was connected with CCD sensor and a computer by light guides. QE value was calculated by the quantum yield measurement software.

3. RESULTS AND DISCUSSION

3.1. The Phase Formation. The as-prepared samples of $CaRNb_3O_{10}$ (R = La, Sm, Eu, Gd, Dy, Er, Yb, or Y) were identified by powder X-ray diffraction measurements as shown in Figure 1. All the patterns have the same profiles with triple perovskite-like structures, which match well with PDF2 standard cards No: 49-0684 selected in the International Centre for Diffraction Data (ICDD) database; the results are in good agreement with the reported data,[28] demonstrating pure crystalline phases.

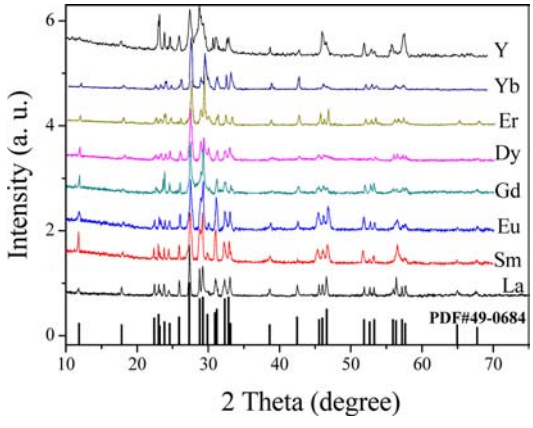

Figure 1. XRD patterns of $CaRNb_3O_{10}$ (R = La, Sm, Eu, Gd, Dy, Er, Yb, Y) together with the standard card of PDF No. 49-0684.

A triple-perovskite $CaRNb_3O_{10}$ is based on an orthorhombic framework of corner-sharing NbO_6 octahedra. The layers consist of three corner-shared NbO_6 chains, R^{3+} and Ca^{2+} ions occupying the 12-coordination sites in the structure.[30] R^{3+} and Ca^{2+} ions can be suggested to randomly occupy the dodecahedral coordination positions in the inner layers; this can be confirmed by the luminescence spectra of structural probe ions of Eu^{3+} in $KCa_2Nb_3O_{10}$: the $^5D_0 \rightarrow {}^7F_0$ transition split into two characteristic luminescence peaks, indicating that Eu^{3+} ions are located at two distinct sites.[29] As a luminescence host, layered perovskite has superiorities, that is, the compound not only shows a high critical concentration quenching but also exhibits a high luminescence brightness. This is because the energy transfer can be restricted within the two-dimensional sublattice.[29]

Figure 2 shows the FE-SEM micrograph of the $CaRNb_3O_{10}$ samples. The obtained micrograph shows that the particles are

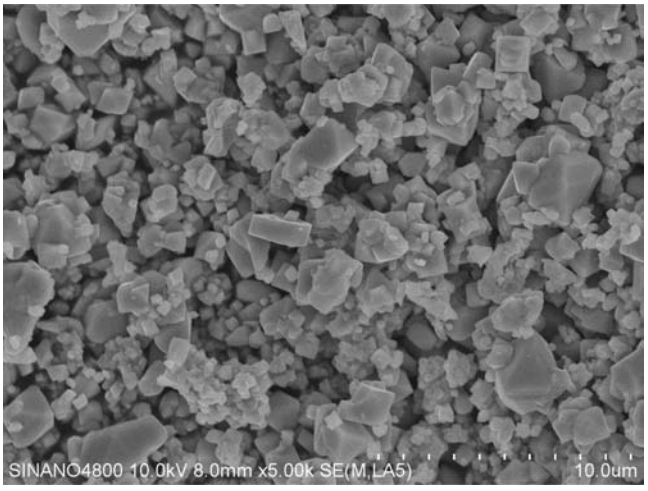

Figure 2. Typical FE-SEM micrographs of the $CaLaNb_3O_{10}$ samples.

agglomerated and have grain or plate-like particles. The average diameter of the grain size is in the range of 500 nm to 3 μm.

3.2. Luminescence of $CaRNb_3O_{10}$ (R = La, Gd, Y, or Yb). The samples of $CaRNb_3O_{10}$ (R = La, Sm, Eu, Gd, Dy, Er, Yb, or Y) have similar UV diffuse reflection spectra. The typical UV diffuse reflection spectrum of $CaLaNb_3O_{10}$ is shown in Figure 3. The adsorption edge is about 280 nm; correspond-

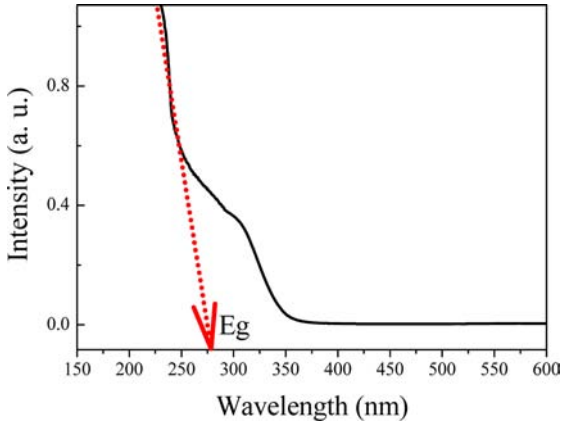

Figure 3. The typical UV−vis diffuse reflectance spectrum of $CaRNb_3O_{10}$ powders measured at room temperature.

dx.doi.org/10.1021/ic401854r | Inorg. Chem. 2013, 52, 10407−10413

ingly, the intrinsic band gap of $CaLaNb_3O_{10}$ is estimated at 4.42 eV. For niobates, the absorption in this spectral region has been attributed to a ligand−metal charge transfer transition (LMCT) from the oxygen ligand to the central niobium atom inside NbO_6 groups.[34]

Figure 4 exhibits the PL excitation and emission spectra together with luminescence decay curves of $CaRNb_3O_{10}$ (R = La, Gd, Yb, or Y). The maximum excitation peak at around 270 nm was observed in the excitation spectra of all samples in Figure 4a. The samples have similar excitation spectra with a broad absorption band from 200 to 300 nm, and the position of the excitation was not appreciably affected by the type of R species. This means that the excitation peak at around 270 nm can be assigned to the excitation of the host layer, presumably, from O 2p to Nb 5d.

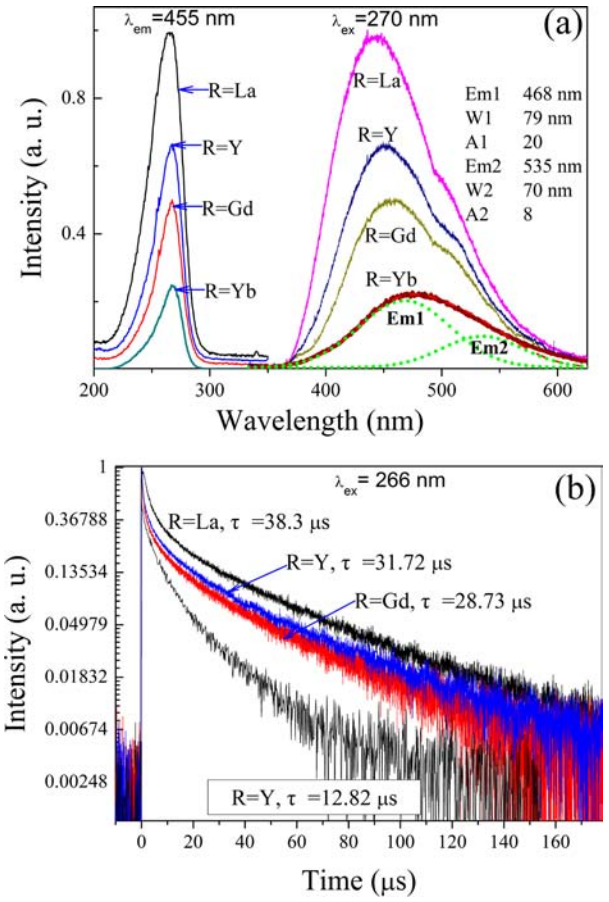

Figure 4. (a) The photoluminescence excitation (em = 455 nm) and emission (ex = 270 nm) spectra of $CaRNb_3O_{10}$ (R = La, Gd, Yb, or Y) at RT; R = Yb was fitted by two Gaussian components with center wavelength Em_1 and Em_2, fwhm W_1 and W_2, and area A_1 and A_2. (b) The luminescence decay curves under the excitation of pulsed 266 nm YAG:Nd laser.

Under 270 nm excitation, there is a broad blue band around 350−620 nm with maximum at 440 nm (R = La), 445 nm (R = Y), 457 nm (R = Gd), and 480 nm (R = Yb). For a niobate, the blue emission is from the CT transition related to the NbO_6 octahedra as efficient luminescence centers of $[NbO_6]^{7-}$ in perovskite layers. Many similar blue emission bands in niobates or tantalites have been reported, such as 442 nm in Bi_3TiNbO_9,[35] 457 nm in $CaNb_2O_6$,[36] 475 nm in $Bi_2SrTa_2O_9$,[15] 425 nm in Sr_3NaNbO_6,[16] 480 nm in $K_{0.98}La_{0.02}Ca_{1.98}Nb_3O_{10}$,[29] 470 nm in $Ba(ZrMgTa)O_3$,[37] 448 nm in $Sr_3Li_6Nb_2O_{11}$,[38] and 460 nm in $Ca_2KNb_5O_{15}$.[39]

It can be noted that each spectrum presents an asymmetry shape, which can be fitted by two Gaussian components as ahown in an example of R = Yb in Figure 4a with center wavelength Em_1 and Em_2, full-width half-maximum (fwhm) W_1 and W_2, and integrated area A_1 and A_2. It has been reported that the blue and the green emission in niobates are due to two different niobate centers, namely, a regular and a defect niobate center.[40] Usually the efficient blue emission originates from the regular niobate center and the weaker green emission from the defect niobate center.[41] For the luminescence of $CaRNb_3O_{10}$ (R = La, Gd, Yb, or Y), we can tentatively assign the blue emission to the intrinsic niobate center and the green emission to a possible defect niobate center; the defects could be formed perhaps by a cation disorder, a niobate center associated with some defects.

Usually, the photoluminescence in highly charged transition metal ion complexes such as titanates, niobates, tantalates, tungstates, and molybdates was proposed to result from a triplet−singlet transition.[42,43] Charge-transfer vibronic excitons from anion groups, defects created by anion deficiencies, or cation disorder with energy states lying within the band gap give rise to luminescence.[16,38] Delocalization of the excited state plays an important role in luminescence, for example, in $LiNbO_3$, $NaNbO_3$, and $KNbO_3$.[44] Structures that exhibit three-dimensional coupling of the d^0 metal ion polyhedra through corner sharing or edge sharing ($CdNb_2O_6$ and $CaTa_2O_6$) show luminescence owing to delocalization of the excited state.[45] Bharathy et al.[16,38] reported blue luminescence in Sr_3NaNbO_6 and Sr_3NaTaO_6 consisting of isolated MoO_4 tetrahedra.[16,38] They also suggested a mechanism as illustrated in Figure 5.

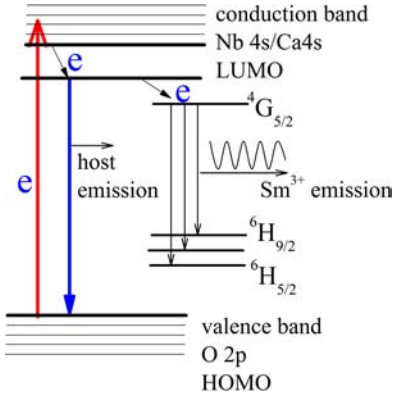

Figure 5. The illustration of the process of photoluminescence in self-activated of $CaRNb_3O_{10}$. This figure was drawn by referring to refs 16 and 38.

After excitation by UV light, an electron is promoted from the valence band or HOMO (a large highest occupied molecular orbital) to the conduction band or LUMO (a lowest unoccupied molecular orbital). There is a nonradiative transfer from the LUMO energy state to an intermediate low-lying LUMO state. A radiative transfer from this intermediate state to the valence band gives rise to the host emission.

The luminescence decay curves of $CaRNb_3O_{10}$ (R = La, Gd, Yb, or Y) under the excitation of the fourth harmonic 266 nm of a pulsed Nd:YAG laser are shown in Figure 4b. The luminescence decay curves exhibit a biexponential feature. Apparently, the emissions show the different luminescence

dx.doi.org/10.1021/ic401854r | Inorg. Chem. 2013, 52, 10407−10413

decay characteristics, indicating the different dynamic emission transition for the emission bands. The average luminescence lifetimes of 38.3, 31.72, 28.73, and 12.82 μs were calculated for R = La, Y, Gd, and Yb, respectively.

The emission spectra have very similar shapes, while the maximum emission peaks and total integrated luminescence intensities (I_{em}) are different from each other; the emission intensity increases from La to Y, Gd, and Yb. The maximum emission wavelengths are at 436, 449.3, 459.3, and 475 nm for R = La, Y, Gd, and Yb, respectively. The excitation band has a peak at 270 nm in the UV region. The Stokes shifts of $CaRNb_3O_{10}$ are estimated to be 14.1 × 10^3 cm^{-1} (R = La), 14.78 × 10^3 cm^{-1} (R = Y), 15.26 × 10^3 cm^{-1} (R = Gd), and 15.98 × 10^3 cm^{-1} (R = Yb).

The luminescence spectra shift brings somewhat different luminescence colors. The CIE (Commission International de l'Eclairage 1931) coordinate values of emissions in $CaRNb_3O_{10}$ (R = La, Gd, Yb, or Y) are shown in Figure 6. It is in the blue

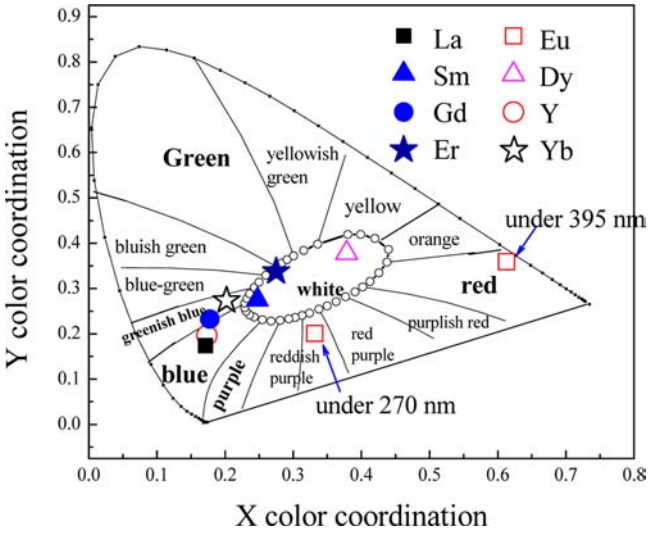

Figure 6. CIE chromaticity coordinates of $CaRNb_3O_{10}$ (R = La, Sm, Eu, Gd, Dy, Er, Yb, or Y).

(R = La and Y) and greenish blue (R = Gd and Yb) region. These CIE values are in agreement with the colors of $CaRNb_3O_{10}$ (R = La, Gd, Yb, and Y) observed visually when illuminated by a hand-held UV lamp (250 nm).

3.3. Luminescence of $CaRNb_3O_{10}$ (R = Sm, Er, or Dy). In $CaRNb_3O_{10}$, the luminescence can be changed with different R elements. Figures 7−10 present the luminescence spectra and luminescence decay curves of $CaRNb_3O_{10}$ (R = Sm, Er, and Dy). They show distinct optical properties due to the difference of the RE ions in the lattices. First, the host luminescence from NbO_6 can be detected in all the samples. The spectra are different from those of $CaRNb_3O_{10}$ (R = Gd, La, Y, or Yb); that is, there are some deep dips and several emission peaks overlapped with the broad emission band. The dips are caused by the absorption from the ground state to upper energy levels of R ions.

The emission spectrum of $CaRNb_3O_{10}$ (R = Sm) under the excitation of 270 nm from CT absorption of NbO_6, is shown in Figure 7a, which comprise both host emission and transition from Sm^{3+} ions. The spectrum under the excitation of interabsorption of Sm^{3+} ions (408 nm) only presents the emission from f → f emission transitions. The broad emission

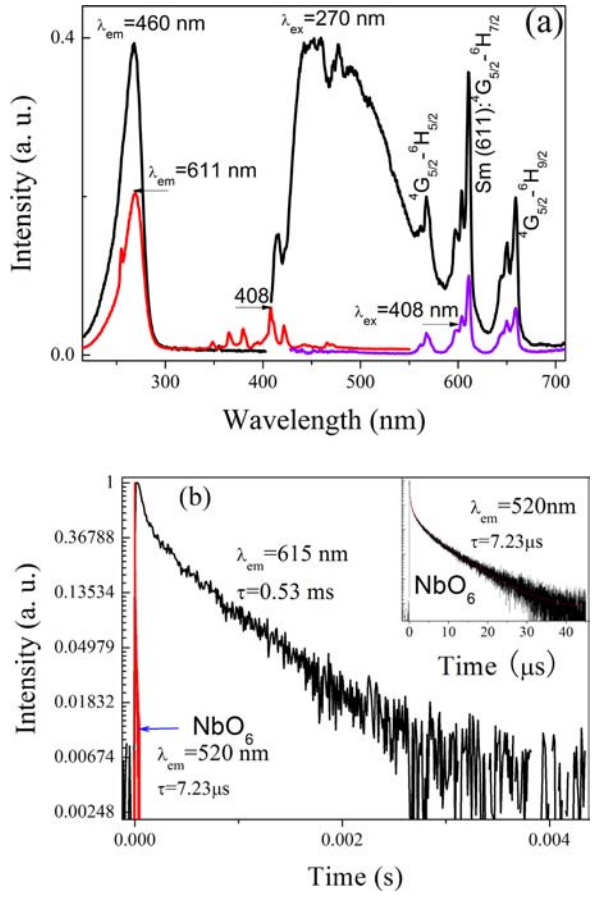

Figure 7. (a) The photoluminescence excitation and emission spectra of $CaSmNb_3O_{10}$ and (b) the luminescence decay curve under the excitation of pulsed 266 nm YAG:Nd laser.

band in Figure 7a is the host emission of NbO_6, and the intense peaks are the f−f transitions of Sm^{3+} with $4f^6$ configuration. The luminescence mechanism is shown in Figure 5. The efficient energy transfer happens from NbO_6 to Sm^{3+} ions.

The excitation spectrum obtained by monitoring the characteristic emission from Sm^{3+} (611 nm, $^4G_{5/2} \rightarrow {}^6H_{7/2}$) has the broad absorption band from CT transition in NbO_6 and the f−f transition of Sm^{3+} itself. Compared with the luminescence decay lifetimes of NbO_6 in $CaRNb_3O_{10}$ (R = Gd, La, Y, or Yb) (tens of microseconds, see Figure 4b), the decay gets faster, 7.23 μs in Figure 7b.

The emission spectra of $CaRNb_3O_{10}$ (R = Er) excited by 270 and 380 nm are displayed in Figure 8a. It was found that the sample emits blue emission from NbO_6 along with luminescence peaks at wavelength 530 and 550 nm, which are attributed to the Er^{3+}: $^2H_{11/2} \rightarrow {}^4I_{15/2}$ and $^4S_{3/2} \rightarrow {}^4I_{15/2}$ transitions, respectively.

Figure 9 is the PL spectra and decay curve of $CaRNb_3O_{10}$ (R = Dy). Except for the broad emission bands from CT transition in NbO_6, the intense line at 575 nm is attributed to the electric dipole transition ($^4F_9 \rightarrow {}^6H_{13}$) of Dy^{3+} and has similar intensity with the magnetic dipole transition (485 nm, $^4F_9 \rightarrow {}^6H_{15/2}$). This indicates that the lack of inversion symmetry in the structure is weaker. The lifetime of 575 nm emission from Dy^{3+} is 4.2 μs as shown in Figure 9b.

Similar excitation spectra phenomena can be found in Figures 7 (R = Sm^{3+}), 8 (R = Er^{3+}), and 9 (R = Dy^{3+}) suggesting that efficient excitation for the emission is in the

dx.doi.org/10.1021/ic401854r | Inorg. Chem. 2013, 52, 10407−10413

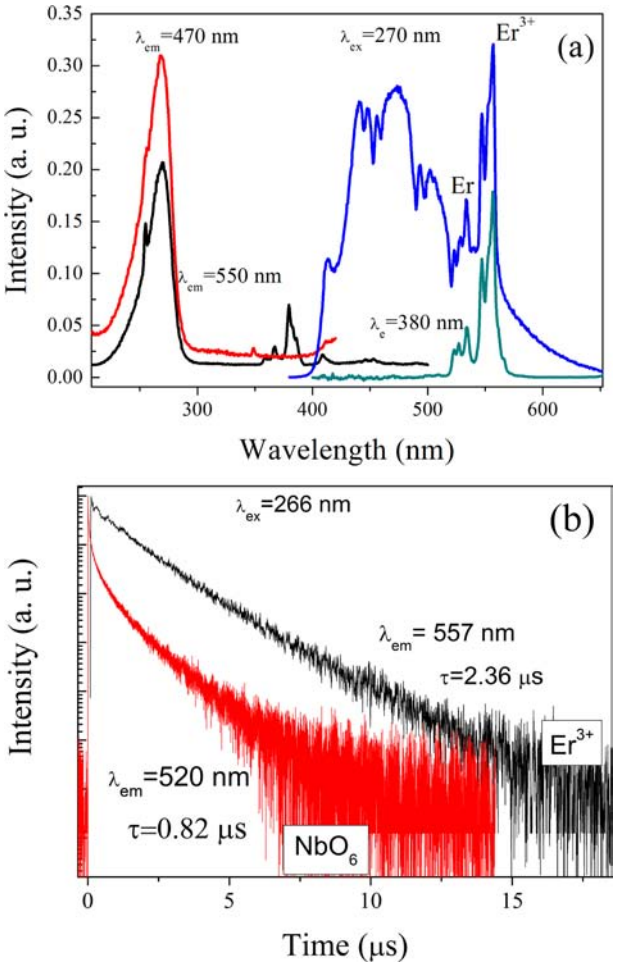

Figure 8. (a) The photoluminescence excitation and emission spectra of $CaErNb_3O_{10}$ and (b) the luminescence decay curve under the excitation of pulsed 266 nm YAG:Nd laser.

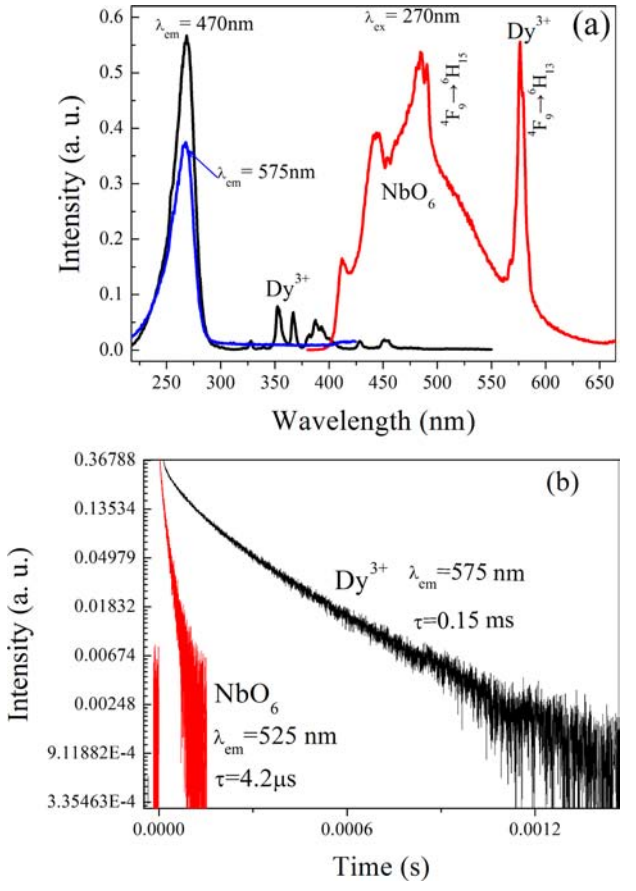

Figure 9. (a) The photoluminescence excitation and emission spectra of $CaDyNb_3O_{10}$ and (b) the luminescence decay curve under the excitation of pulsed 266 nm YAG:Nd laser.

region of UV-light, 200−300 nm. The decay lifetimes for blue emission from NbO_6 in the samples of $CaRNb_3O_{10}$ (R = Sm, Er, or Dy) are about 1 order of magnitude lower than those obtained from R = Gd, La, Y, or Yb. This indicates an energy transfer process from Nb−O CT to R^{3+} ions. Consequently, the spectra of $CaRNb_3O_{10}$ (R = Sm, Er, or Dy) consist of the emission peak from R^{3+} ions and a broad band from NbO_6 groups. The CIE color-coordinate values were calculated to be ($x = 0.247$, $y = 0.275$) for R = Sm, ($x = 0.378$, $y = 0.379$) for R = Dy, and ($x = 0.275$, $y = 0.337$) for R = Er. It can be found in Figure 6 that the values are located in the white color region. This indicates that $CaRNb_3O_{10}$ (R = Sm, Er, or Dy) could be a single-phase phosphor for white lighting under UV light excitation.

3.4. Luminescence of $CaRNb_3O_{10}$ (R = Eu). Figure 10 shows the PL spectra and decay curves of $CaRNb_3O_{10}$ (R = Eu). The excitation spectrum by monitoring the $^5D_0 \rightarrow {}^7F_2$ emission (613 nm) of Eu^{3+} ions consists of a broad band and some sharp lines. The broad excitation band centered at 270 nm can be attributed to O → Nb CT transition. In the range from 350 to 550 nm, there are characteristic intraconfigurational 4f−4f transitions of Eu^{3+}: 395 nm ($^7F_0 \rightarrow {}^5L_6$), 464 nm ($^7F_0 \rightarrow {}^5D_2$), and 535 nm ($^7F_1 \rightarrow {}^5D_1$). This well matches with the output wavelength of near-UV or blue LED chips in phosphor-converted W-LEDs.

The decay lifetime of the $^5D_0 \rightarrow {}^7F_2$ luminescence at 613 is calculated to be 0.52 ms; however, the intrinsic emission from NbO_6 is greatly depressed with a fast decay lifetime of 5.17 μs shown in Figure 10b. The result shows that the efficient energy transfer happens from NbO_6 to Eu^{3+} ions.

The characteristic red emission of the Eu^{3+} ion is observed under excitation at 270 and 394 nm. The luminescence spectrum excited by 395 nm shows the $^5D_0 \rightarrow {}^7F_{1-4}$ transitions. However, under excitation of 270 nm, the emission in Figure 10a ranging from 400 to 700 nm has both the host emission of NbO_6 and the intense peaks centered at 590 nm ($^5D_0 \rightarrow {}^7F_1$) and 613 nm ($^5D_0 \rightarrow {}^7F_2$) of the f−f transitions of Eu^{3+} with $4f^6$ configuration. Consequently the luminescence of $CaRNb_3O_{10}$ (R = Eu) can be changed under different excitation wavelength. Under UV light, the CIE coordinates ($x = 0.331$, $y = 0.201$) in reddish purple region; while the luminescence under 395 nm presents red color with CIE values of ($x = 0.613$, $y = 0.361$).

Table 1 summarizes the luminescence data in $CaRNb_3O_{10}$ (R = La, Sm, Eu, Gd, Dy, Er, Yb, or Y) such as excitation and emission wavelength, CIE color coordinates, luminescence centers, and luminescence intensity. What should be specially noted is the luminescence intensity, which is normalized to that in $CaRNb_3O_{10}$ (R = La). The luminescence was depressed in the case of R = Sm, Gd, Dy, Er, Yb, and Y; however, the luminescence intensity was increased in R = Eu by the excitation with both UV and near UV light. The strongest luminescence intensity is obtained for $CaRNb_3O_{10}$ (R = Eu) excited at 270 nm even if there exists energy transfer from

dx.doi.org/10.1021/ic401854r | Inorg. Chem. 2013, 52, 10407−10413

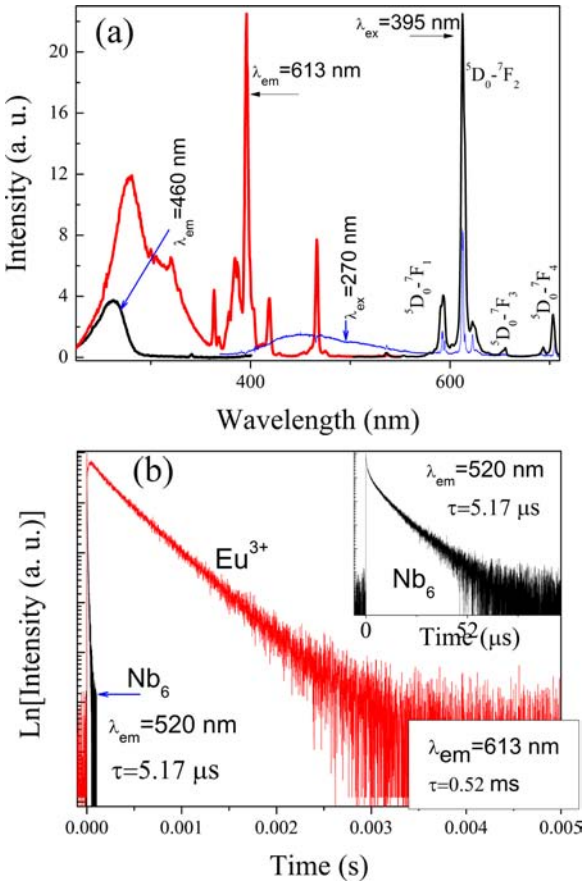

Figure 10. (a) The photoluminescence excitation and emission spectra of $CaEuNb_3O_{10}$ and (b) the decay curve under the excitation of pulsed 266 nm YAG:Nd laser.

NbO_6 to Eu^{3+} ions. This change of luminescence intensities was confirmed by photoluminescence QE values as listed in Table 1. The maximum measured QE value (excitation at 270 nm) at room temperature is 42.0% in $CaEuNb_3O_{10}$. This is higher than that of $Y_2O_2S:Eu^{3+}$ (35% excitation by 317 nm)[46] and YAG:Eu^{3+} (40% excitation by 254 nm).[47] The phosphor can be suggested to be an excellent candidate for materials in lighting and display.

3.5. The XEL Spectra. The luminescence of $CaRNb_3O_{10}$ (R = La, Sm, Eu, Gd, Dy, Er, Yb, or Y) was detected under the excitation by X-rays. It is interesting that the luminescence intensities under X-ray are different from those under UV light. Only luminescence of the samples of R = La, Gd, and Y can be detected at room temperature.

Figure 11 shows the XEL spectra of $CaRNb_3O_{10}$ (R = La, Gd, and Y), which were compared with that of $Bi_4Ge_3O_{12}$

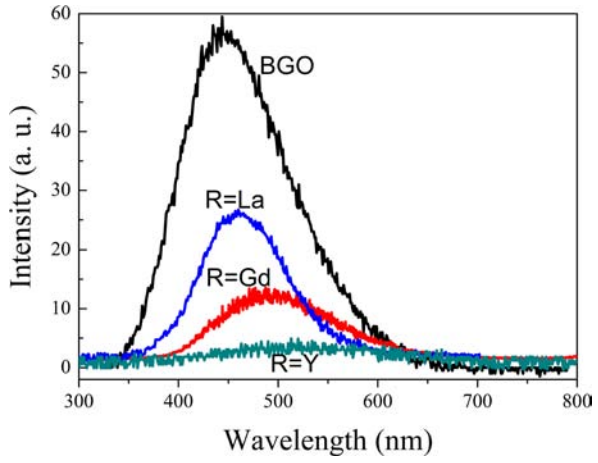

Figure 11. X-ray-excited UV emission spectra of $CaRNb_3O_{10}$ (R = La, Gd, Y) and a comparison with the emission spectrum of BGO.

(BGO) powders under the same conditions. Under the excitation with X-ray, the emission spectra of the two phosphors keep the same profile as that under 270 nm excitation. By comprising the integral emission intensities, the light yields of $CaRNb_3O_{10}$ (R = La) and $CaRNb_3O_{10}$ (R = Gd) are 39.5% and 21.8% of that of $Bi_4Ge_3O_{12}$ powders, respectively. The results in our experiments indicate that these niobates are not effective candidates as potential XEL materials or scintillators.

4. CONCLUSIONS

In summary, $CaRNb_3O_{10}$ (R = La, Sm, Eu, Gd, Dy, Er, Yb, or Y) has a layered perovskite-type structure with an estimated band gap energy of 4.42 eV. The niobates present tunable luminescence colors with different R ions in the host, for example, blue (R = La or Y), greenish blue (R = Gd or Yb), white (R = Sm, Er, or Dy), reddish purple (R = Eu, under UV light, 200−300 nm), and red (R = Eu, under near-UV light, around 400 nm). The samples $CaRNb_3O_{10}$ (R = La, Gd, Yb, or Y) have an excitation band from 200 to 300 nm with a maximum wavelength at 270 nm. Under UV light, $CaRNb_3O_{10}$ (R = La, Gd, Yb, or Y) presents blue luminescence from the CT transition related to the NbO_6 octahedra with average luminescence lifetimes of tens of microseconds. As a stoichiometric component in the $CaRNb_3O_{10}$ host, an activator rare earth ion such as Sm, Er, Dy, or Eu shows a high critical

Table 1. The Main Luminescence Data of $CaRNb_3O_{10}$ (R = La, Sm, Eu, Gd, Dy, Er, Yb, or Y)

R	excitation (nm)	emission (nm)	intensity[a]	CIE (*x*, *y*)	QE (%)	luminescence centers
La	270	436	1	(0.172, 0.173)	31	NbO_6
Y	270	449	0.70	(0.174, 0.197)	25	NbO_6
Gd	270	459	0.62	(0.177, 0.232)	22	NbO_6
Yb	270	475	0.30	(0.202, 0.273)	16	NbO_6
Eu	270	460, 613	1.93	(0331, 0.201)	42	Eu^{3+}, NbO_6
	395	613	1.75	(0.613, 0.361)		Eu^{3+}
Sm	270	460, 611	0.48	(0.247, 0.275)	21	Sm^{3+}, NbO_6
Dy	270	470, 575	0.47	(0.378, 0.379)	13	Dy^{3+}, NbO_6
Er	270	470, 550	0.37	(0.275, 0.337)	11	Dy^{3+},NbO_6

[a]Integrated intensity normalized to that of $CaLaNb_3O_{10}$.

dx.doi.org/10.1021/ic401854r | *Inorg. Chem.* 2013, 52, 10407−10413

quenching concentration and exhibits a high luminescence brightness. $CaRNb_3O_{10}$ (R = Sm, Er, Dy, or Eu) show emission from f → f transitions, which overlapped with the broad band from NbO_6 luminescence; of all the compounds, $CaRNb_3O_{10}$ (R = Eu) shows the strongest luminescence brightness. Moreover, the excitation band of $CaRNb_3O_{10}$ (R = Eu) well matches with the output wavelength of near-UV or blue LED chips in phosphor-converted W-LEDs. Under X-ray, only the luminescence from $CaRNb_3O_{10}$ (R = La, Gd, or Y) can be detected at room temperature.

AUTHOR INFORMATION

Corresponding Authors

*Hyo Jin Seo. E-mail: hjseo@pknu.ac.kr. Tel: +82-51-629 5568. Fax:+82-51-6295549.

*Ynalin Huang. E-mail: huang@suda.edu.cn. Fax: +86-512-65880089.

Notes

The authors declare no competing financial interest.

ACKNOWLEDGMENTS

This research was supported by Basic Science Research Program through the National Research Foundation of Korea (NRF) funded by the Ministry of Science, ICT & Future Planning (NRF-2013-R1A1A2009154), and by A Project Funded by the Priority Academic Program Development of Jiangsu Higher Education Institutions (PAPD).

REFERENCES

(1) Yang, T.; Claridge, J. B.; Rosseinsky, M. J. *Inorg. Chem.* **2013**, *52*, 3795−3802.

(2) Peel, M. D.; Thompson, S. P.; Aladine, A. D.; Ashbrook, S. E.; Lightfoot, P. *Inorg. Chem.* **2012**, *51*, 6876−6889.

(3) Viciu, L.; Caruntu, G.; Royant, N.; Koenig, J.; Zhou, W. L.; Kodenkandath, T. A.; Wiley, J. B. *Inorg. Chem.* **2002**, *41*, 3385−3388.

(4) Ochi, M.; Yamada, I.; Ohgushi, K.; Kusano, Y.; Mizumaki, M.; Takahashi, R.; Yagi, S.; Nishiyama, N.; Inoue, T.; Irifune, T. *Inorg. Chem.* **2013**, *52*, 3985−3989.

(5) Shiro, K.; Yamada, I.; Ikeda, N.; Ohgushi, K.; Mizumaki, M.; Takahashi, R.; Nishiyama, N.; Inoue, T.; Irifune, T. *Inorg. Chem.* **2013**, *52*, 1604−1609.

(6) Luo, K.; Hayward, M. A. *Inorg. Chem.* **2012**, *51*, 12281−12287.

(7) Oliva, C.; Allieta, M.; Scavini, M.; Biffi, C.; Rossetti, I.; Forni, L. *Inorg. Chem.* **2012**, *51*, 8433−8440.

(8) Neilson, J. R.; Kurzman, J. A.; Seshadri, R.; Morse, D. E. *Inorg. Chem.* **2011**, *50*, 3003−3009.

(9) Tsujimoto, Y.; Yamaura, K.; Muromachi, E. T. *Appl. Sci.* **2012**, *2*, 206−219.

(10) Zhang, W.; Ye, H. Y.; Graf, R.; Spiess, H. W.; Yao, Y. F.; Zhu, R. Q.; Xiong, R. G. *J. Am. Chem. Soc.* **2013**, *135*, 5230−5233.

(11) Song, J. H.; Im, J.; Androulakis, J.; Malliakas, C. D.; Li, H.; Freeman, A. J.; Kenney, J. T.; Kanatzidis, M. G. *J. Am. Chem. Soc.* **2012**, *134*, 8579−8587.

(12) Doan, P.; Gooch, M.; Tang, Z. J.; Lorenz, B.; Möller, A.; Tapp, J.; Chu, P. C. W.; Guloy, A. M. *J. Am. Chem. Soc.* **2012**, *134*, 16520−16523.

(13) Mitchell, J. F.; Millburn, J. F.; Medarde, M.; Short, S.; Jorgensen, J. D.; Fernandez-Diaz, M. T. *J. Solid State Chem.* **1998**, *141*, 599−603.

(14) Kobayashi, Y.; Tian, M. L.; Eguchi, M.; Mallouk, T. E. *J. Am. Chem. Soc.* **2009**, *131*, 9849−9855.

(15) Ida, S.; Ogata, C.; Unal, U.; Izawa, K.; Inoue, T.; Altuntasoglu, O.; Matsumoto, Y. *J. Am. Chem. Soc.* **2007**, *129*, 8956−8957.

(16) Bharathy, M.; Rassolov, V. A.; zur Loye, H. C. *Chem. Mater.* **2008**, *20*, 2268−2273.

(17) Yamaura, K.; Shirako, Y.; Kojitani, H.; Arai, M.; Young, D. P.; Akaogi, M.; Nakashima, M.; Katsumata, T.; Inaguma, Y.; Muromachi, E. T. *J. Am. Chem. Soc.* **2009**, *131*, 2722−2726.

(18) Ida, S.; Okamoto, Y.; Matsuka, M.; Hagiwara, H.; Ishihara, T. *J. Am. Chem. Soc.* **2012**, *134*, 15773−15782.

(19) Tong, H.; Umezawa, N.; Cao, J. Y.; Li, P.; Bi, Y. P.; Zhang, Y. J.; Ye, J. H. *J. Am. Chem. Soc.* **2012**, *134*, 1974−1977.

(20) Dion, M.; Ganne, M.; Tournoux, N.; Revez, J. *Chim. Miner.* **1984**, *21*, 92−103.

(21) Dion, M.; Ganne, M.; Tournoux, M. *Mater. Res. Bull.* **1981**, *16*, 1429−1435.

(22) Constantino, V. R. L.; Bizeto, M. A.; Brito, H. F. *J. Alloys Compd.* **1998**, *278*, 142−147.

(23) Fukuoka, H.; Isami, T.; Yamanak, S. *J. Solid State Chem.* **2000**, *151*, 40−45.

(24) Jacobson, A. J.; Lewandowski, J. T.; Johnson, J. W. *J. Less-Common Met.* **1986**, *116*, 137−146.

(25) Han, Y. S.; Choi, S. H.; Jang, J. U.; Kim, D. Q. *J. Solid State Chem.* **2001**, *160*, 435−443.

(26) Nakato, T.; Kuroda, K. *Eur. J. Solid State Inorg. Chem.* **1995**, *32*, 809−818.

(27) Kudo, A.; Tanaka, A.; Domen, K.; Maruya, K.; Aika, K.; Ohnishi, T. *J. Catal.* **1988**, *111*, 67−76.

(28) Uma, S.; Golpalakrishnan, J. *J. Solid State Chem.* **1993**, *102*, 332−339.

(29) Bizeto, M. A.; Constantino, V. R. L.; Brito, H. F. *J. Alloys Compd.* **2000**, *311*, 159−168.

(30) Machida, M.; Mitsuyama, T.; Ikeue, K.; Matsushima, S. *J. Phys. Chem. B* **2005**, *109*, 7801−7806.

(31) Schaak, R. E.; Mallouk, T. E. *Chem. Mater.* **2002**, *14*, 1455−1471.

(32) Sato, T.; Fukugami, Y.; Shu, Y. *Scr. Mater.* **2001**, *44*, 1905−1910.

(33) Kudo, A.; Sakata, T. *J. Phys. Chem.* **1996**, *100*, 17323−17326.

(34) Blasse, G.; Grabmaier, B. C. *Luminescence Materials*; Springer: Heidelberg, 1994.

(35) Ma, Q.; Zhou, Y. Y.; Lu, M. K.; Zhang, A. Y.; Zhou, G J. *Mater. Chem. Phys.* **2009**, *116*, 315−318.

(36) Hsiao, Y. J.; Liu, C. W.; Dai, B. T.; Chang, Y. H. *J. Alloys Compd.* **2009**, *475*, 698−701.

(37) Yanagida, T.; Fujimoto, Y.; Yokota, Y.; Yoshikawa, A.; Kuretake, S.; Kintaka, Y.; Tanaka, N.; Kageyama, K.; Chani, V. *Opt. Mater.* **2011**, *34*, 414−418.

(38) Bharathy, M.; Rassolov, V. A.; Park, S.; zur Loye, H. C. *Inorg. Chem.* **2008**, *47*, 9941−9945.

(39) Yin, X.; Shi, L.; Wei, A.; Wan, D. Y.; Wang, Y. M.; Huang, F. Q. *J. Solid State Chem.* **2012**, *192*, 182−185.

(40) Macke, A. J. H. *J. Solid State Chem.* **1976**, *19*, 221−226.

(41) Wiegel, M.; Hamoumi, M.; Blasse, G. *Mater. Chem. Phys.* **1994**, *36*, 289−293.

(42) Ilangovan, R.; Balakumar, S.; Subramanian, C. *Mater. Sci. Technol.* **1999**, *15* (1), 32−136.

(43) Vikhnin, V. S.; Eglitis, R. I.; Kapphan, S. E.; Borstel, G.; Kotomin, E. A. *Phys. Rev.* **2002**, *B65*, No. 104304.

(44) Wiegel, M.; Emond, M. H. J.; Stobbe, E. R.; Blasse, G. *J. Phys. Chem. Solids* **1994**, *55*, 773−778.

(45) Blasse, G. *Struct. Bonding (Berlin)* **1980**, *42*, 1.

(46) Huang, Y.; Nakai, Y.; Tsuboi, T.; Seo, H. J. *Opt. Express* **2011**, *19*, 6303−6311.

(47) Uhlich, D.; Huppertz, P.; Wiechert, D. U.; Jüstel, T. *Opt. Mater.* **2007**, *29*, 1505−1509.